Shear lag in bolted tension members at elastic and yielding loading conditions

Fathy A. Abdelfattah and Mohamed S. Soliman
Civil Eng. Dept., Faculty of Engineering at Shobra, Zagazig University, Cairo, Egypt

This study measures the effects of shear lag on bolted tension members loading capacity at elastic and yielding conditions. Nonlinear finite element analysis was used. The model includes steel strain hardening effects. Comparing the obtained results with experimental results presented in the literature validated the finite element model. Members of single and double angles, I-shape and channels are considered. The results show that shear lag exists at elastic and yielding loading conditions. Size and dimensions of member section, connection details and material strength effect shear lag magnitude. The results are compared against the guidance given in the different codes of practice. The authors proposed modification to the formulas provided in the Egyptian code (2001) and British standards BS5950 (1985) to include connection length when evaluating tension member loading capacity.

تقيس هذه الدر اسه القدرة التحميلة لأعضاء الشد الموصلة بالمسامير في مرحلة السلوك المرن و اللدن و تأثير تباطئي القص عليها. تم استخدام طريقة العناصر المحدودة. تم تمثيل سلوك الحديد بطريقة لا خطية تطابق سلوكه الناتج من اختبارات الشد. التوافق بين النتائج المستخرجة من طريقة العناصر المحدودة و النتائج العملية المنشورة في الدوريات تأكد سلامة التمثيل المستخدم في هذه الدراسة. تم تطبيق الدراسة على عدة أشكال لقطاعات أعضاء الشد. النتائج توضح تواجد تباطئي القص و تأثيره على القدرة التحميلية سواء في مرحلة السلوك المرن و اللدن. مقاس و أبعاد قطاع عضو الشد بالإضافة إلى تفاصيل الوصلة و نوع الحديد المستخدم هي عوامل تؤثر على قيمة تباطئي القص.تم مقارنة النتائج المستخرجة من طريقة العناصر المحدودة وتلك الناتجة من تطبيق المعادلات في المواصفات المختلفة. تم اقتراح لتعديل المعادلات في المواصفات المصرية و البريطانية لإدخال تأثير طول الوصلة عند حساب القدرة التحميلية لأعضاء الشد.

Keywords: Shear lag, Tension members, Stress concentration

1. Introduction

Current design methods of tension members are based on the assumption that the nominal design strength will develop in a uniform pattern through the critical net section of the member. In practice, tension members of single and double angles are usually connected to gusset plate through one leg. The eccentricity of fasteners at end connections introduces eccentric tension load into the member. The induced stresses and strains at the critical net section, in the direction of the applied tension, are not equal and their distribution is not uniform. Stresses are concentrated in the connecting leg. Stresses in the unconnected leg become less in value and not uniform. This phenomenon is termed " shear lag in tension member".

Chesson and Munse [1] presented review of the literature about shear lag in tension members. Further, they reported the experimental results of thirty specimens having different sections. They considered angles connected back-to-back to a common gusset plate forming star shape and built up sections of box and I shapes. The measurements of the strains in the angles and the webs of all the considered sections showed that shear lag exist. Munse and Chesson [2] introduced empirical reduction factor *U*. It is used in the design process to include the effect of shear lag. The effective net area A_e is used instead of the net area A_n at the critical net section.

$$A_e = A_n \; U, \tag{1}$$

$$U = (1 - e_x / L). \tag{2}$$

Where e_x is the distance from the center of the member area to the face of the gusset plate and L is the length between the first and last

rows of bolts. The full examination and justification of U was reported by Chesson [3]. This factor is used later in the American specifications AISC [4-6] for the design of tension member.

Kulak and Wu [7] reported the experimental results of 24 specimens of single and double angles subjected to tension loads. This number of tests, as they indicated, is limited in comparison to the variables considered. They used the numerical model proposed by Wu and Kulak [8] to obtain a prediction of members' ultimate loads. Because of the large amount of computational time required, only five of the test specimens were modeled analytically. Epstein and Aiuto [9] presented a design method by using moment and axial force interaction equations to account for moment and shear lag effects in tension members. The moment is produced due to the eccentricity of the applied tension and depends on the connection geometry and rotational stiffness. Shear lag exists also in welded tension members. Easterling and Giroux [10] reported the results of 27 tests. They concluded that shear lag controls member strength when longitudinal welds is used. For members connected with transverse welds, weld shear will be the controlling limit.

2. Shear lag at yielding

In all the studies presented in the literature, shear lag was measured at ultimate loading conditions. This failure mode agrees with that considered in some of codes of practice as the AISC-LRFD [6]. However, yielding of the net section is the failure criterion in allowable stress methods of design provided in the Egyptian codes ECP [11], and AREA [12]. This also applies to the method of defining tension member capacity in BS5950 [13]. Yielding at the net section in a bolted tension member would initiate at the edges of bolts' holes and extend gradually through the net section. This mechanism may not continue until the full yielding of the net section because of (i) shear lag and (ii) steel strain hardening. At loads less than or equal to the yielding load P_y, stresses may approach its ultimate value at regions around bolts' holes initiating mechanism of local failure. Stresses at outstanding leg may not reach the design strength value or even be in the opposite direction; i.e. compression.

3. Objectives of the study

The objectives of this study are to:

1. Know the effect of shear lag on stresses distributions at elastic and plastic loading conditions.
2. Measure shear lag effects at yielding and/or the initiation of local failure on the loading capacity of tension members.
3. Assess the efficiency of the different shapes of tension members' sections.
4. Measure the validity of the different recommendations given in different codes for evaluating shear lag at yielding loading conditions.

4. Loading capacity

In this study the finite element method is used to obtain the loading capacity of tension members, $P_{F.E.}$. It is considered as that load, which cause any of the following conditions:

1. Full yielding at the critical net section.
2. The stresses induced at bolts holes' edges at the critical net section approach the ultimate strength value.

Satisfying the first condition agrees with the concept used in allowable stress method of design in the Egyptian code ECP [11]. When the later condition occur, the factor of safety against $P_{F.E.}$ would provide suitable margin to avoid crack initiation at bolts holes edges. Crack propagation may lead to failure before yielding of the full net section.

5. Finite element model

Nonlinear finite element analysis is carried out for modeling shear lag in tension members. Members of single angle, double angles symmetrically connected to gusset plate between them, I-shape and Channels are considered. The ANSYS 5.4 computer program for finite element analysis was used. For members of single angle, both the gusset plate and the angle are modeled using about 2500 shell elements, fig. 1-a. The shell element has

6 degrees of freedom at each node; translations in the nodal *X, Y* and *Z* directions

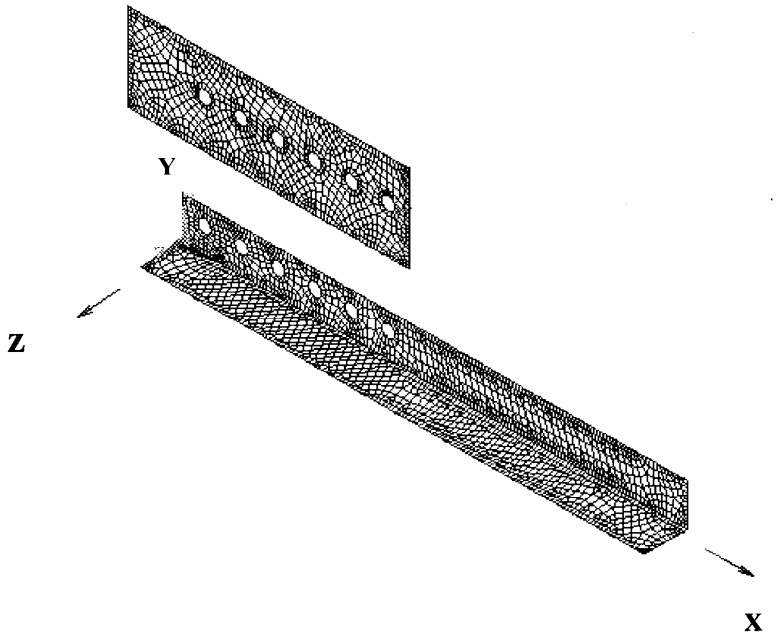

Fig. 1-a. Finite element mesh.

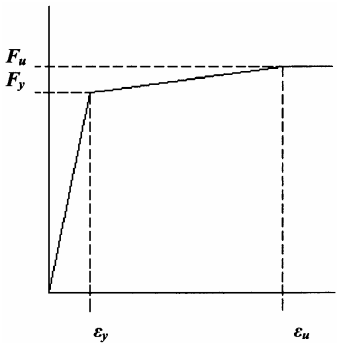

Fig. 1-b. idealized stress-strain curve.

and rotations about the nodal *X, Y* and *Z* axes. The element formulation includes plastisity and large strain capabilities, ANSYS [14]. Only half of the angle length was modelled due to its symmetry about the *Y – Z* plane. The elements at that position were restrained against translation in the *X* axis and rotation about the *Y* and *Z* axes. The gusset plate was modeled having thickness larger than that of the connected leg or legs to it. It was restrained at its remote edge against translation in the *Z* -axis and rotation about the *X* and Y-axes to simulate its continuty in practice to other members. Axial tension force was applied to the gusset plate in the form of concentrated loads. Each bolt hole was defined by 16 node at its circumferance. These nodes were made coinciding in the gusset plate and the connected leg of the angle. The bolts themselves were not modelled. However, their behavoiur was modelled by coupling the degrees of freedom of the first 5 coonsideing nodes at each bolt hole in the angle with their counterpart in the gusset plate. This would not include the interaction of both the bending and shear effects in the bolts body. This is expected to have negligable effect in the results. Only half of the section is modeled for the members of double angles. For members of I sections and channels, quarter of the section is modeled. However, the restraining conditions are modified to simulate the existing symmetry conditions.

Nonlinear stress-strain relationship was used for the steel material. The elastic modulus of elasticity was taken E = 205000 N/mm^2. The multilinear Kinematic hardening option available at ANSYS 5.4 was used to model the plasticity and strain hardening behavior of the steel material, ANSYS [14]. The values of the strength and strain at yielding and ultimate of the steel used are specified; F_y,, ε_y , F_u and ε_u, respectively. This produced tangent modulus $E_t = (F_u - F_y) / (\varepsilon_u - \varepsilon_y)$ for the

stress-strain curve portion between yielding and failure, fig. 1-b.

For comparison purpose, steel sections complying with the American standard shapes were used. It was found that most of the angles are available in four different values for the thickness. Angles of unequal legs are also available with different four values for the ratio between the lengths of the two legs. This facilitates examining the effects of these two parameters. Steel types complying with the Egyptian codes and the American specifications are used.

6. Comparison between experimental and numerical results

Fig. 2 presents the load-elongation relationship for specimen S9 from the experimental work of Kulak and Wu [7]. The original figure was magnified and the different points of the relationship were measured and then plotted. The finite element method was used to model the behaviour of S9. The obtained load-elongation relationship is also presented in fig. 2. The modeled length of the member in the finite element analysis was made as short as possible to reduce the number of elements in the mesh. This increased its axial stiffness and caused the limited differences in values between the two relations in the elastic range. The actual yield and ultimate tensile strength values, obtained from tensile tests, of the steel in S9 were not available in [7]. The nominal values were reported and used in the finite element analysis. This reason in addition to the method of modeling steel strain hardening caused the differences between the two

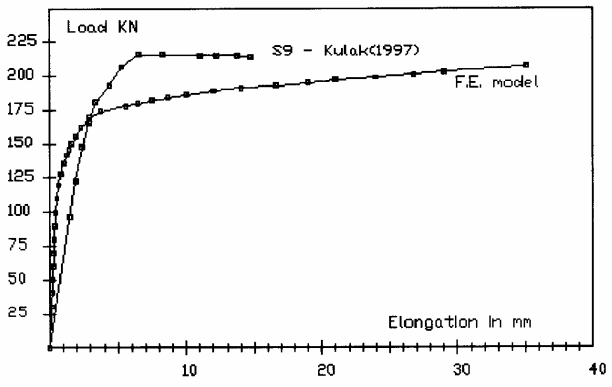

Fig. 2. Comparison between the experimental and the finite element results.

relations at failure. In general, the two relations show nearly the same manner of behavior and good agreement specially up to yielding.

7. Effect of shear lag on stresses distributions

Fig. 3-a shows the stress distribution for a member of double angles of size 127x76x6.4 mm. The member is connected by 3 bolts of diameter d = 22mm at the short leg of the angle. The gauge is equal $2d$ while the distance between the bolts s is equal to 3d. The applied load P_1 = 0.45 P_y where $P_y = A_n * F_y$. This value of P_1 is equal to the allowable load when using the formula provided in the ECP [11] and BS 5950 [13] to include the effect of shear lag. The values of the stress in the direction of the applied load f_x are plotted in terms of the ratio f_x/ f_n where f_n is the nominal stress, $f_n = P_1 / A_n$. The values of the equivalent stress to the yielding stress ratio f_e/ F_y are plotted in fig. 3-b. Shear lag exists at elastic loading conditions. The values of f_x through the connecting leg is about double the nominal stress f_n. The magnitude of f_e is nearly equal to the yielding stress at bolt hole edges. Part of the unconnected leg is subjected to compression stress.

Figs. 4-a and 4-b show the values of f_x/ f_n and f_e/ F_y for the same connection when P_2=0.72 P_y. Both shear lag and modeling of the steel strain hardening produced the obtained stress patterns. The values of f_e vary between F_u and F_y through the connecting leg. The stress at bolt hole edge is maximum and equals F_u. This would initiate local failure mechanism at that area. This load is considered as the tension member loading capacity; i.e. $P_{F.E.}= P_2$. The unconnected leg can be divided into three parts. The area

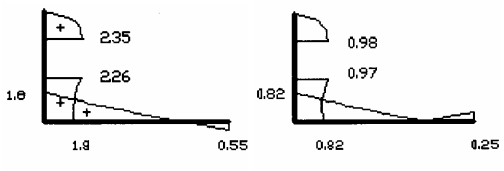

(a) Values of f_x / f_n (b) Values of f_e / f_y

Fig. 3. Stresses distribution at load P_1 = 0.45 P_y.

beside the connecting leg is subjected to tension stress where the values of f_e are nearly equal to F_y. In the area at leg toe, the values of f_e are nearly equal to F_y. This is due to the induced compression stress. In the middle area, the stress f_x varies from tension to compression. The ratio of ($P_{F.E.}$ / P_1) equals 1.6. This value is nearly equal to the factor of safety used in ECP [11] for the design of tension members when shear lag does not exist.

8. Tension members of single and double angles

This section is devoted to members of single angle and members of back-to-back double angles connected symmetrically to gusset plate between them. These types of members are commonly used in trusses. The following parameters are considered:

i. Ratio of connected leg length to unconnected length; a / b.
ii. Ratio of connected leg length to leg thickness; a / t.
iii. Distance between bolts; s.
iv. Ratio of the ultimate to the yield tensile strength values; F_u / F_y.
v. Number of bolts in one row of connections; n.

The connections considered to examine the variables in points i to iv are made of two bolts only. This would magnify the effect of shear lag and indicates clearly the effect of changing the values of the different variables considered above.

8.1. Effect of a / b

The angles in table 1 have the same thickness t and connected leg length a. The sole variable considered is the length of the unconnected

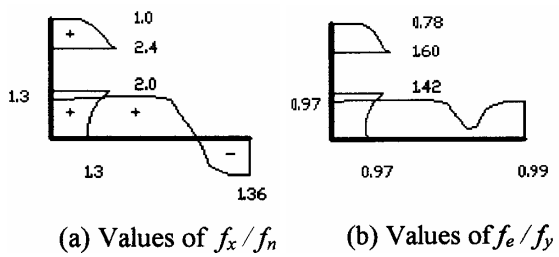

(a) Values of f_x / f_n (b) Values of f_e / f_y

Fig. 4. Stresses distribution at load P_2 = 0.72 P_y.

outstanding leg, b. The change of b caused changes in A_n within a range of 170%. The ratio a / b varied between 0.6 and 1.5. This covers the range of a / b values for the different sizes of angles available in practice. The obtained values of $P_{F.E.}$ / P_y are found very sensitive to the changes in a / b. However, limited changes occurred in $P_{F.E.}$ The maximum difference in $P_{F.E}$ value between S1 and S4 is 10.6 kN while a / b and A_n are nearly doubled. This is explained as follows. When b is increased, the eccentricity of the applied load and A_n are increased. These two factors have opposite effects. The first would elevate the degree of shear lag magnitude and creates regions of stress concentrations at bolts holes edges. As a consequence, the stresses would approach the ultimate strength at lower applied loads. This would dismantle the effect of net area increase.

8.2. Effect of a / t

The considered angles in table 2 have equal legs' lengths. The ratio of a / t are varied from 6 to 15.8. This changed the angles net area within a range of 150%. The values of $P_{F.E.}$ are found very sensitive to the changes in A_n. However, the changes in $P_{F.E.}/P_y$ are found within a limited range. This is explained as follows. The variation of angles legs' thickness caused limited changes in the position of the angles center of gravity. The eccentricity of the applied tension for the different cases is nearly equal. This produced nearly the same magnitude of shear lag and hence that limited change in $P_{F.E.}/P_y$.

8.3. Distance between bolts, s

Members of single and double angles of size 76 x 76 x 12.7 are used. Bolts pitch s was changed from 3 Φ to 6 Φ. The ratio of $P_{F.E.}/P_y$ is found proportional to s, fig. 5. The results are justified by the following explanation. The load transferred through the first bolt in the connection would induce unequal stresses at that section due to shear lag. The stresses are then redistributed through the distance s. The use of relatively small s would not allow the

full redistribution of the stresses before the second bolt. This magnifies the shear lag at the second bolt. The results in general indicates the importance of including this parameter when defining shear lag magnitude.

Table 1
Loading capacity of tension members with different values of a/b

Specimen	Member		a/b	$P_{F.E.}/P_y$	Connection details
	Type	Angle size*			
S1	Single angle	127x76x6.4	0.6	0.54	a/t =11.87
S2		102x76x6.4	0.75	0.62	a = 76 mm
S3		76x76x6.4	1.0	0.75	d =22mm
S4		76x51x6.4	1.5	0.9	Φ =24mm
D1	Double angles	127x76x6.4	0.6	0.54	n =2
D2		102x76x6.4	0.75	0.63	s =3.5d
D3		76x76x6.4	1.0	0.76	g =2d
D4		76x51x6.4	1.5	0.91	F_y=250 N/mm²
					F_u=400 N/mm²

* All the dimensions are in mm

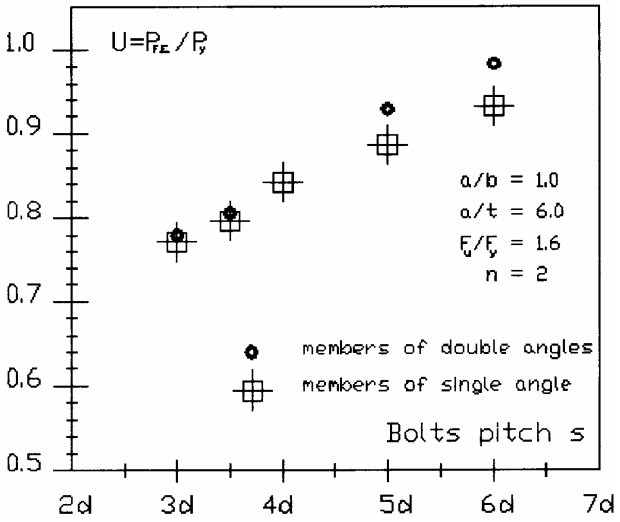

Fig. 5. Effect of distance between bolts on $P_{F.E.}/P_y$ ratio.

8.4. Steel strength values F_Y and F_U

Fig. 6 presents the results of $P_{F.E.}/P_y$ when using different types of steel having different values of F_y, F_u and F_u/F_y ratio. All the steel types specified in the Egyptian code [11] and those designated A36, A242 and A441 in the American specifications and allowed to be used in the AISC-LRFD [6] are considered. Single angles of size 76x76x12.7 mm are used. The different steel types are arranged in the abscissa according to the values of F_u/F_y. The ratio of $P_{F.E.}/P_y$ is found proportional to F_u/F_y. The increase in F_u/F_y would provide wide range between the yield and ultimate strength of the steel material. This would accommodate shear lag effect at regions of stress concentration. This reduces the effect of shear lag on tension member loading capacity.

8.5. Bolts number n

Members of single and double angles of size 76 x 127 x 6.4 are used. The results obtained are presented in fig. 7. The $P_{F.E.}/P_y$ ratio is found proportional to n. Increasing the number of bolts would reduce the load transferred by each bolt. Hence, relatively less unequal strains and stresses are expected to induce through the angle section. This would elevate tension members' efficiency. This behavior is more pronounced in members

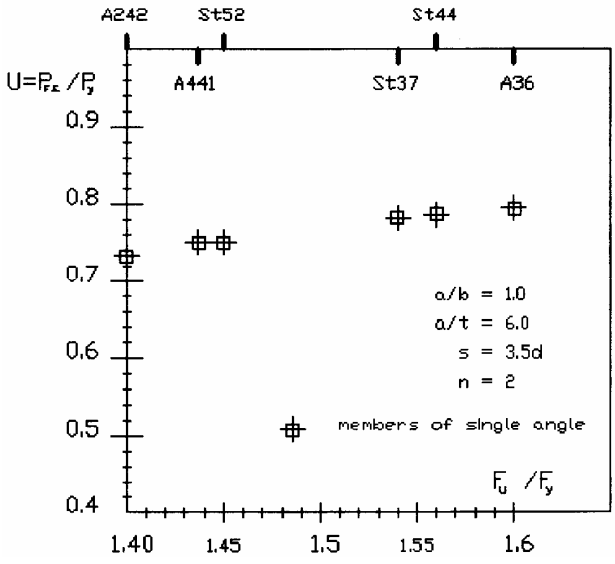

Fig. 6. Effect of using steel materials with different *Fu/Fy* ratio on *PF.E./Py* values.

Table 2
Loading capacity of tension members with different values of *a/t*

Specimen	Member		*A/t*	$P_{F.E.}/P_y$	Connection details
	Type	Angle size*			
S5	Single angle	76x76x12.7	6.0	0.79	*a/b*=1.0 *a* = 76 mm *d* =22mm Φ =24mm *n* =2 *s* =3.5d *g* =2d F_y=250 N/mm² F_u=400 N/mm²
S6		76x76x9.5	8.0	0.77	
S7		76x76x6.4	11.87	0.75	
S8		76x76x4.8	15.8	0.74	
D5	Double angles	76x76x12.7	6.0	0.81	
D6		76x76x9.5	8.0	0.77	
D7		76x76x6.4	11.87	0.76	
D8		76x76x4.8	15.8	0.74	

* All the dimensions are in mm

of double angles. Fig. 8 shows the results for members of single angles of size 76x76x6.4 and 76x76x12.7. The ratio of $P_{F.E.}/P_y$ reached unity in most of these cases. This does not mean that shear lag does not exist. At areas of stress concentration, the stresses exceeded F_y but still less than F_u. However, at other areas stresses did not reach the yielding strength value.

8.6. Comparison between sections of single and double angles

Tables 1 and 2 show that counterpart members of single and double angles are affected in the same mannar and by the same magnitude of shear lag. Herbrant and Demel [15] and Kulak and Wu [7] reached to the same conclusion. This applies to all the cases considered in this study except when *s* and *n*

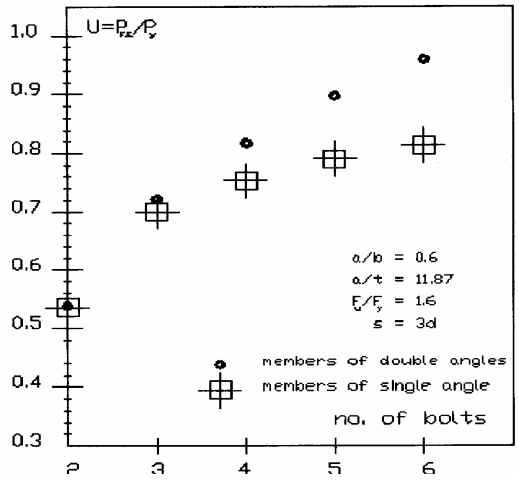

Fig. 7. Effect of bolts number on *PF.E./Py* ratio.

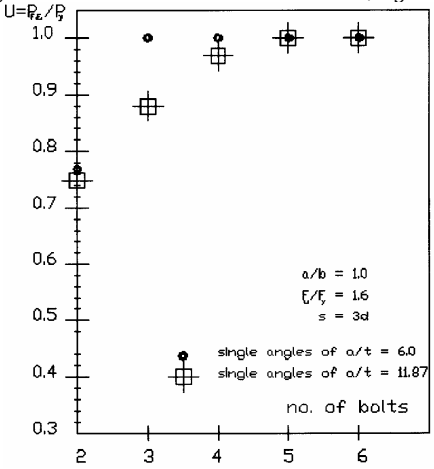

Fig. 8. Effect of bolts numbers on *PE.E./Py* ratio.

are varied. The magnitude of shear lag for single angle members in figs. 5 and 7 are more pronounced than their counterparts of double angles. The increase of *s* and/or *n* enhanced the loading capacity for the members of double angles. The results in general show that the problem of shear lag can be classified as a local bending problem. Each angle in double angle members seems to act individually rather than as a part of a rigid body.

9. Members of channels and I-sections

Two channels were used for tension members' sections in table 3. Three different forms, named A, B and C, are considered as follows:

A: Two gusset plates are connected to the flanges of the channels.

Table 3
Loading capacity of tension members with different cross section forms

Specimen	Member size*	a/b	t_c/t_o	$P_{F.E.}/P_y$	Connection details **	Members cross section forms
A1	2 channels C250 x 45	0.6	0.65	1.0	d=22mm n= 6	Form A 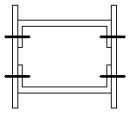 For specimens A1, A2 and A3
B1	Properties: Mass=45Kg/m D=254mm B_f=76mm t_f=11.1mm t_w=17.1mm	1.67	1.54	1.0	For specimens A1, B1 and C1	
C1		1.67	1.54	1.0		
A2		0.6	0.65	0.68	d=30mm n=3	Form B  For specimens B1, B2 and B3
B2		1.67	1.54	1.0	For specimens A2, B2 and C2	
C2		1.67	1.54	1.0		
A3	2 channels C250 x 22	0.6	1.82	0.96	d=22mm n=3	Form C 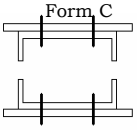 For specimens C1, C2 and C3
B3	Mass=22Kg/m t_f=11.1mm t_w=17.1mm	1.67	0.55	0.78	For specimens A3, B3 and C3	
C3		1.67	0.55	0.77		
I1	S shape S460 x 104	0.35	0.97	1.0	d=24mm n=6	Form I  For specimens I1, I2 and I3
I2	Mass=104Kg/m'	0.35	0.97	1.0	d=30mm n=4	
I3	S shape S460x81 Mass=81.4Kg/m	0.35	1.5	1.0	d=24mm n=5	

* Steel strength considered are F_y=250 N/mm^2 and F_u=400 N/mm^2
** In all the connections s =3d, Φ =d+2mm and g =2d

B: The channels are connected at the web to the opposite sides of one gusset plate.
C: Each channel is connected at the web to a different gusset plate.
Tension members of I-sections are also considered. Two digits name each specimen in table 3. The first refers to the section form. The second digit refers to the connection details. The values of $P_{F.E.}/P_y$ equal unity for A1, B1 and C1. This means that A_e is equal to A_n and the sections can resist the yielding load with out initiation of local mechanism of failure. However, this is not the rule. The results show that A2 is less efficient than B2 and C2. On the contrary, A3 is more efficient than B3 and C3. The results can be analyzed by making analogy between quarter of the members' section and members of single angles. In A2, the ratios of the thickness and length of the connected leg to those of the unconnected leg; i.e. a/b and t_c/t_o, are less than those of B2 and C2. The channel flange in this case is a and b is half the web depth. In A3, t_c/t_o = 1.82 as the thickness of the flange is about double that of the web. This elevated the member efficiency and raised $P_{F.E.}/P_y$ value to approach 0.96. The results of B3 and C3 confirm the effects of t_c/t_o ratio on shear lag magnitude.

For comparison purposes, two members of single angles named *L1* and *L2* having the same values of a, b, t_c , t_o, n, s and d of A1 and A2, respectively, are analyzed. The values of $(P_{F.E.})_{L1}$ / $(P_{F.E.})_{A1}$ and $(P_{F.E.})_{L2}$ / $(P_{F.E.})_{A2}$ are 0.69 and 0.9, respectively. The results indicate the significance of the symmetry conditions provided due to the use of channel section in A1 and A2. The use of I-sections in I1, I2 and I3 produced value for $P_{F.E.}/P_y$ equal unity although the connections details are different. The thickness of the flange is greater than that of the web in most of I-sections. This applies to all sections complying with American standard S shapes, the IPE sections

of the German specifications DIN 997 [16] and universal beams of the British standards BS4 [17].

Table 4
Formulas available in codes of practice to calculate effective net area

Code	Effective net area for bolted members		Notes
	Single angles, T sections, and channels	Double angles back to back	
ECP [11] BS 5950 [13]	$A_e=a_1 + a_2 (3a_1 / (3a_1 +a_2))$	$A_e=a_1 + a_2 (5a_1 / (5a_1 +a_2))^*$	a_1= net area of connected leg a_2= gross area of unconnected leg
AREA [12] AASHTO [19]	$A_e = a_1 + (1/2)\, a_2$	----------	
AISC-LRFD [6] AISC-ASD [4]	$A_e= A_n (1 - e_x /L)$		A_n= net area at critical cross section L= connection length e_x= distance from bolt plane to the center of the cross section area.
Env 1993-1-1:1992 [20]	$A_e = A_n \beta$		A_n= net area at critical cross section β vary between 0.4 and 0.7 depending on bolts number and spacing
CAN/CSA-S16.1-94 [21]	$A_e = A_n \beta_n$		A_n= net area at critical cross section β_n vary between 0.6 and 0.85 depending on section shape and bolts number and spacing

* For BS 5950 (1985) only.

10. Codes of practice

The concept of using effective net area A_e in the design process is implemented in codes of practice to include the effect of shear lag. Table 4 presents the formulas provided in different eight codes of practice. It worth noting that ECP [11] considers tension members unsymmetrical connected to gusset plates. Different cases of single angles and back-to-back double angles connected to one side of gusset plate or section are considered. However, the case of double angles symmetrically connected to gusset plate that passes between them was not included. This case is dealt with in BS 5950 [13], and as explained in text books as that of the British Steel Construction Institute and edit by Owens and Knowles [18], using the formula in table 4 of double angles. Figs. 9 and 10 show the relations of $(A_e)_{code}/(A_e)_{F.E.}$ for the members of single and double angles considered in this study and the different variables. The values of $(A_e)_{F.E.}$ are calculated as the ratio of $P_{F.E.}/f_y$. The formulas in ECP [11], BS 5950 [13], AREA [12] and AASHTO [19] produced relations of the same pattern but not the same magnitude. The concept of the formulas is the same. It considers the net area of the connected leg and ratio of the area of the unconnected leg. It does not consider the connection length. Table 5 compares between the mean, variance and standard deviation of the different values of $(A_e)_{code}/(A_e)_{F.E.}$. The formulas in ECP [11] and BS 5950 [13] under estimate the effect of shear lag. The variance and standard deviation values are relatively large in comparison to those of the AISC [4,6].

11. Proposed modifications to formulas in ECP (2001) and BS 5950 t

The authors proposed the following modifications to the formulas in the ECP [11] and BS 5950 [13]. The results obtained from the finite element analysis are measured against these formulas. A new term W is obtained to include the effect of s and n in the calculation of A_e as follows:

$$W = j \ \mathrm{LN} \ (K * L / b). \quad (3)$$

Where J = 0.5 and K = 5.8 for members of single angles and J = 0.8 and K = 3.12 for members of double angles. The term L represents the connection length as $L = s\,(n - 1)$ and b is the length of the unconnected leg of the angle. The term W is implemented in the formulas as follows:

For members of single angles;

$$A_e = a_1 + (3a_1 / (3a_1 + a_2)) * a_2 * W . \quad (4\text{-a})$$

Table 5
The average, variance and standard deviation for the different values of $(A_e)_{code}/(A_e)_{F.E.}$ ratio

Code	Members of single angle			Members of double angles		
	Average	Variance	St. dev*.	Average	Variance	St. dev*.
ECP [11]	1.06	0.1122	0.1396	--	--	--
BS 5950 [13]				1.075	0.096	0.164
AREA [12] AISC [6]	1.866	0.0055	0.067	0.8311	0.00002	0.0545
Formulas (4-a) and (4-b)	1.043	0.001	0.0345	0.9615	0.0023	0.0426

*Standard deviation

For members of double angles;

$$A_e = a_1 + (5a_1 / (5a_1 + a_2)) * a_2 * W . \quad (4\text{-b})$$

Formulas (4-a) and (4-b) are used to calculate the values of A_e for the members and connections considered in this study. For comparison, the values of $(A_e) / (A_e)_{F.E.}$ are calculated and plotted in figs. 9 and 10. The results in table 5 show remarkable enhancement for the average, variance and standard deviation of $(A_e)/(A_e)_{F.E}$ values when calculated using formulas 4-a and 4-b. This emphasis on the concept of including the connection length when defining shear lag magnitude in tension members. For more validation, the authors suggest that formulas (4-a) and (4-b) should be measured against greater number of results.

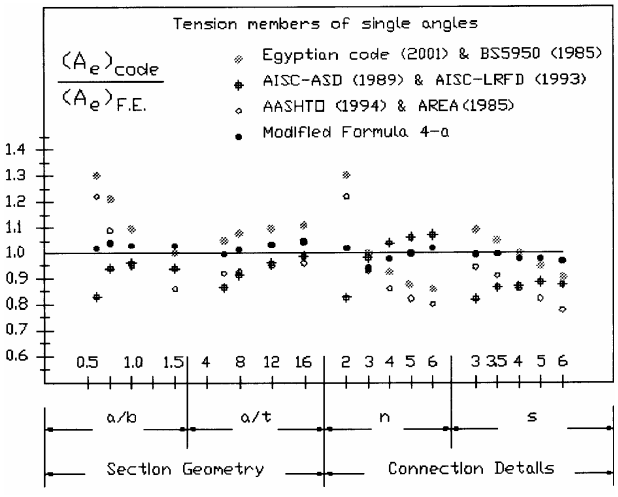

Fig. 9. Values of $(A_e)_{code}/ (A_e)_{F.E.}$ obtained using different codes of practice for members of single angle.

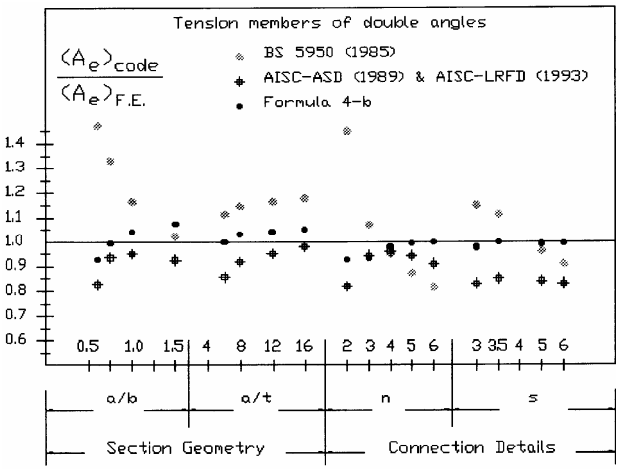

Fig. 10. Values of $(A_e)_{code}/ (A_e)_{F.E.}$ obtained using different codes of practice for members of single angle.

12. Conclusions

Shear lag exists at elastic and yielding loading conditions. Stress distribution is different to that assumed in design methods. At allowable load, tension stress f_x in the connecting leg may reach double the nominal stress value f_n , fig. 3-a. At loads less than or equal to the yielding load, the stress value approach the ultimate tensile strength, fig. 4-b. This occurs at bolts holes edges. Shear lag magnitude is effected by shape of tension member section and the dimensions of the different elements in the section in addition to connection details. The loading capacity for members of single angles and members of back to back double angles connected

symmetrically to gusset plate between them are affected in the same manner and by the same magnitude of shear lag, tables 1 and 2. The ratio of the connected leg length to that of the unconnected leg length a/b affects shear lag values to a relatively high degree, table 1. The ratio of the connected leg length to the angle thickness a/t is another parameter, table 2. This applies also to members consisting of two channels, table 3. I-section is seen to be the most efficient sections in resisting tension loads when connected through the flanges. The number of bolts n and the distance between them s are found to effect shear lag, figs. 5, 7 and 8. The authors proposed modifications to the formulas in the Egyptian codes [11] and British standards BS 5950 [13] to include n and s when calculating tension members loading capacity. The results show remarkable enhancement.

Notations

A_e	is the effective net area,
A_n	is the net area at critical section,
a	is the length of connected leg,
B_f	is the flange width,
b	is the length of unconnected leg,
D	is the channel depth,
d	is the bolt diameter,
E	is the modulus of elasticity,
e_x	is the distance from the center of member area to the face of gusset plate,
F_y	is the yield strength,
F_u	is the ultimate strength,
f_e	is the equivalent stress,
f_n	is the nominal stress,
f_x	is the tension stress in the direction of the applied load,
G	is the gauge distance,
J, K, W, U	are factors,
L	is the distance between first and last bolt in row,
n	is the number of bolts in one row,
$P_{F.E.}$	is the tension member loading capacity,
P_y	is the yielding load,
s	is the distance between bolts,
t	is the thickness of angle legs,
t_c, t_o	are the thicknesses of connected and unconnected legs, respectively,
t_f, t_w	are the thickness of Flange and web, respectively,
Φ	is the bolt hole diameter, and
$\varepsilon_y, \varepsilon_u$	is the strain at yielding and ultimate strength values, respectively.

References

[1] E. Chesson, Jr. and W. H., Munse, "Riveted and bolted joints: truss-type tensile connections.", J. Struct. Engrg., ASCE, Vol. 89 (1), pp. 67-106 (1963).

[2] W. H. Munse, and E. Chesson, Jr., "Riveted and bolted joints: net section design," J. Struct. Engrg., ASCE, Vol. 89 (1), pp. 107-126 (1963).

[3] E. Chesson, Jr., "Behavior of large riveted and bolted structural connections," Thesis presented to the university of Illinois, at Urbana, U.S.A., in partial fulfillment of the requirements for the degree of Doctor of Philosophy (1959).

[4] Specification for structural steel buildings-allowable stress design and plastic design, American Institute of Steel Construction (AISC), Chicago (1989).

[5] Load and resistance factor design specification for structural steel buildings, American Institute of Steel Construction (AISC), Chicago (1993).

[6] Load and resistance factor design specification for structural steel buildings, American Institute of Steel Construction (AISC), Chicago, Dec. 27 (1999).

[7] G. L. Kulak, and E. Y. Wu, "Shear lag in bolted angle tension members," J. Struct. Engrg., ASCE, Vol. 123 (9), pp. 1144-1152 (1997).

[8] Y. Wu, and G. L. Kulak, "Shear lag in bolted single and double angle tension members", Struct. Engrg. Rep. (187), Dept. of Civ. Engrg., Univ. of Alberta, Edmonton, Canada (1993).

[9] H. I. Epstein, and L. D., Aiuto, "Using moment and axial interaction equations to account for moment and shear lag effects in tension members", Engrg. J.,

AISC, Vol. 39 (2), pp. 67-76, Second quarter (2002).
[10] W. S. Easterling, and L. G., Giroux, "Shear lag effects in steel tension members," Engrg. J., AISC, Vol. 30 (3), pp. 77-89, Third quarter (1993).
[11] Egyptian code of practice for steel construction and bridges (Allowable stress design), Code No. 205, Ministerial Decree No. 279 – 2001, Permanent Committee for the Code of Practice for Steel Construction and Bridges, Housing and Building Research Center, Cairo, Egypt (2001).
[12] Specifications for steel railway bridges AREA, American Railway Engineering Association (1985).
[13] British Standards BS 5950: Structural use of steel works in building: Part 1, British Standard Institute, London, UK (1985).
[14] ANSYS User's Manual for Revision 5.0, Vol. 1, Procedures (1992).
[15] F. Hebrant, and L. Demol, "Tensile tests on riveted connection of rolled sections made of steel A37", Acier, Stahl. Steel, Vol. 20 (4), pp. 178-184 (1955).
[16] German specification DIN 997, Deutsches Institut fur Normung e. V., Berlin (1970).
[17] British Standards BS 4: Structural steel sections: Part 1: Specification for hot rolled sections, British Standard Institute, London, UK (1980).
[18] G. W. Owens, and P. R. Knowles, Steel Designer's Manual, fifth edition, The Steel Construction Institute, London (1994).
[19] Standard specifications for highway bridges AASHTO, American Association of state highway and transportation officials, Washington, D. C. (1994).
[20] Eurocode 3: Design of steel structures-Part 1.1: General rules and rules for buildings Env 1993-1-1: 1992, European Committee for Standardization, Brussels (1993).
[21] National Standard of Canada CAN/CSA-S16.1-94, Candian Standards Association, Canada (1994)

Received March 11, 2003
Accepted July 9, 2003